Spectral coherence and time-domain transport of waves in random media

Gregory Samelsohn,[1,*] Valentin Freilikher,[2] and Motti Haridim[1]
[1]*Department of Communication Engineering, Holon Institute of Technology, Holon 58102, Israel*
[2]*The Jack and Pearl Resnick Institute of Advanced Technology, Department of Physics, Bar-Ilan University, Ramat-Gan 52900, Israel*
(Received 26 January 2008; published 3 December 2008)

An original approach is developed for the description of spectral coherence and time-domain transport of wave fields scattered in random media. This approach accounts explicitly for the correlation properties of the disorder and is universal with respect to the dimensionality of the system. Specifically, a two-frequency mutual coherence function is evaluated by using a procedure of embedding the initial Helmholtz equation into an auxiliary problem of a directed wave propagating in a higher-dimensional space. The resulting Schrödinger-like equation is solved perturbatively by means of a cumulant path integral technique. Mean intensity profiles and temporal moments of a narrowband wave packet scattered in a random medium are calculated by using the Fourier transformation of the coherence function. The theory describes the ballistic to diffusive transition in wave transport, and is consistent with experimental results. Since the coherence function is expressed via an arbitrary form power spectrum, the results obtained open a new avenue for studying wave transport in anisotropic and/or fractally correlated systems.

DOI: 10.1103/PhysRevE.78.066602 PACS number(s): 43.20.+g, 42.25.Dd, 41.20.Jb

I. INTRODUCTION

In this work, we study spectral coherence and time-domain transport of wave fields scattered in random media. Specifically, we evaluate the two-frequency mutual coherence function (sometimes called the frequency field-field correlator), which is an important quantity in itself, and is intimately related, via an appropriate Fourier transform, to the mean shape of pulsed waves propagating in random media [1]. Correspondingly, there is a large variety of applications which cover both direct and inverse problems dealing with light propagation in the atmosphere and biological tissues, underwater acoustics and seismology, radio waves in the ionosphere, interstellar plasmas, etc. The study of spectral coherence is especially important in the context of time-reversal experiments, where self-averaging of the wave field and the related effects of spatial focusing and time compression can be achieved only when the spectrum of the pilot signal is much wider than the coherence bandwidth of the medium [2].

When considering the propagation of wave fields in random media, one usually deals with two extreme regimes for which the analysis of wave transport may be essentially simplified. The first is quasiballistic propagation in which the wave is scattered mostly in the direction of its initial propagation, and the cumulative deflection angle is rather small. In this case, the Helmholtz equation can be reduced to a parabolic wave equation in which backscattering is completely neglected, and the lateral diffusion of the wave energy is described in the paraxial approximation [1]. Such waves are usually called *directed* waves. Since the resulting parabolic equation has the form of the Schrödinger equation in quantum mechanics, an efficient tool to construct the solution for the statistical moments of the field is by means of a path integral technique [3]. There exists a vast literature considering the two-frequency coherence function of directed waves (see, e.g., Refs. [4–7]). In particular, in our recent paper [7], the coherence function was calculated by use of a cumulant expansion of the corresponding path integral.

When the distance of propagation in the random medium increases or the scattering becomes stronger, a crossover from ballistic to isotropic diffusion regime usually occurs. The regime of *diffuse* waves corresponds to propagation distances which are much larger than the mean free path that defines a natural scale of scattered wave isotropization [8]. A conventional way to describe related phenomena is to use the diffusion equation, which may be obtained from the ladder approximation of the Bethe-Salpeter equation, provided the disorder is δ correlated in the configuration space [9]. The latter condition is satisfied, formally, for small-scale inhomogeneities where the correlation scale is much smaller than the radiation wavelength. In the more general, less restrictive case, we arrive at the radiative transfer equation (RTE) capable of accounting consistently for the disorder statistics in both small- and large-scale inhomogeneities, thus filling the gap between the ballistic and diffusion regimes in wave propagation. Recently, an essential progress has been achieved in deriving the improved version of RTE for waves propagating in random media with resonant pointlike scatterers [10]. However, the physics of RTE (even if the latter is derived somehow from the wave equations) is based on the energy balance which is natural, e.g., for neutrons, but not for waves where coherent effects may play an important role. Indeed, it has been predicted theoretically and confirmed experimentally that the scattering of waves in the backward direction may be enhanced as compared to the value given by RTE (the effect of weak localization) [8]. This effect has recently been analyzed in a number of papers, with a rich collection of the results that now constitute a well-developed theory. Moreover, as was first predicted by Anderson for electron waves [11], under some conditions, radiation in disordered media cannot propagate at all, the statement that constitutes the essence of the so-called strong localization effect [8].

*samelsohn@hit.ac.il

Usually, the presence of inelastic scattering, partial coherence of the source, and the finite size of the sample wash out the coherence of waves for long trajectories, inevitably leading to a classical radiative transfer at large (in terms of the scattering mean free path) distances. However, under the conditions of quenched disorder, a nonclassical, phase coherent diffusion could take place even when the Anderson localization is absent. For example, recently observed stimulated emission in random lasers with coherent feedback [12] provides a direct evidence of a limited applicability of the diffusion approximation in strongly scattering media. The coherent feedback in such systems arises from photon transport along closed loop paths formed by the recurrent scattering [13,14], the mechanism that is fully neglected in the framework of the classical diffusion paradigm.

In view of relative efficiency of the evolutional type parabolic equation in studying directed waves, it is reasonable to search for a similar formulation valid in the general case, including the regime of wave localization. A possible way to transfer to an evolutional type equation is to use Fock's embedding procedure, according to which the solution of the Helmholtz equation is presented as an integral over pseudotime, the integrand being a solution of the generalized parabolic Schrödinger-like equation [15]. Here, for auxiliary directed waves, the medium is assumed to have no variation of the refractive index along the pseudotime coordinate. The latter point makes the problem quite different from the usual memoryless Markov model typical of directed wave propagation. However, a perturbative path integral technique developed in Refs. [15–17] allows the transport properties of various disordered systems to be studied consistently by taking into account their microstructure statistics.

In this work, we extend the above approach to the case of the two-frequency mutual coherence function and temporal behavior of wave fields propagating in random media, mainly in the intermediate regime lying between ballistics and diffusion, which up to now has remained practically unexplored. Although scattering is rather strong in this regime, coherent effects may be of great importance. In particular, a special attention should be paid to coexistence of ballistic and diffuse waves in scattering experiments, which is manifested, for example, in a bimodal form of the photon time-of-flight distributions for ultrashort laser pulses [18]. These phenomena can be used in an effective imaging through turbid media, where a variety of different modalities, such as time-gating techniques or optical coherence tomography, have been recently proposed [19,20]. As we will show, the results obtained in this paper from the first principles, without any resort to phenomenological models such as RTE, predict the two-scale structure of both the coherence function and the impulse response, and are fully consistent with known experimental results obtained in this intermediate scattering regime. Since the coherence function is expressed via an arbitrary form power spectrum, the results obtained in the work open a new avenue for studying wave transport in anisotropic and/or fractally correlated systems.

The outline of the paper is as follows. In Sec. II, we present a mathematical model for the wave propagator and define the statistics of the random medium. In Sec. III, we briefly describe the derivation procedure (more details may be found in Appendixes A and B), and arrive at a general result for the coherence function given in the form of a weighted integral over the power spectrum of the disorder. Wave transport in the time domain, including the calculation of the first temporal moments of a narrowband wave packet, is considered in Sec. IV. The results obtained are applied in Sec. V to three-dimensional isotropic systems with Gaussian and exponential correlation functions. Finally, Sec. VI contains a summary and concluding remarks.

II. PROPAGATOR MODELING

To describe time-harmonic wave propagation in scattering media, we start with the Helmholtz equation for the Green's function $G(\mathbf{r}|\mathbf{r}_0)$,

$$\nabla^2 G(\mathbf{r}|\mathbf{r}_0) + k^2[1+\tilde{\varepsilon}(\mathbf{r})]G(\mathbf{r}|\mathbf{r}_0) = -\delta(\mathbf{r}-\mathbf{r}_0), \quad (2.1)$$

where $\mathbf{r}$ denotes the position vector in an m-dimensional space (m can range from 1 to 3), k is the wave number of a homogeneous "reference" medium, and $\varepsilon(\mathbf{r})=1+\tilde{\varepsilon}(\mathbf{r})$ is the relative permittivity distribution, such that $\tilde{\varepsilon}(\mathbf{r})$ may be considered as a random scattering potential. It is assumed that $\tilde{\varepsilon}(\mathbf{r})$ is a Gaussian random field with zero mean value $\langle\tilde{\varepsilon}(\mathbf{r})\rangle=0$. Hereafter, the angular brackets mean ensemble average. For statistically homogeneous fluctuations, the correlation function depends only on the distance between the corresponding points

$$B_\varepsilon(\mathbf{r}) = \langle\tilde{\varepsilon}(\mathbf{r}')\tilde{\varepsilon}(\mathbf{r}'+\mathbf{r})\rangle. \quad (2.2)$$

In its turn, the power spectrum of the scattering potential is given by

$$\Phi_\varepsilon(\mathbf{K}) = (2\pi)^{-m}\int d\mathbf{r}\,\exp(-i\mathbf{K}\cdot\mathbf{r})B_\varepsilon(\mathbf{r}). \quad (2.3)$$

The most straightforward way to study the statistical moments of the wave field is based upon presenting the unknown solution of Eq. (2.1) as a functional of the scattering potential, with successive averaging over its fluctuations. To do this it is appropriate to convert the initial problem to some auxiliary, evolutional-type equation that would satisfy the dynamic causality condition [21]. This strategy can be easily accomplished while dealing with directed waves, where the elliptic-type Helmholtz equation can be reduced to a parabolic equation. In order to achieve the same goal when the wave is scattered diffusively in all directions, we resort to another technique. Specifically, according to the Fock's method of proper time [22], we consider an auxiliary problem for a function $g(\mathbf{r},\tau|\mathbf{r}_0,0)$ satisfying the generalized parabolic equation

$$2ik\partial_\tau g + \nabla^2 g + k^2\tilde{\varepsilon}(\mathbf{r})g(\mathbf{r},\tau|\mathbf{r}_0,0) = 0, \quad \tau \geqslant 0, \quad (2.4a)$$

$$g(\mathbf{r},0|\mathbf{r}_0,0) = \delta(\mathbf{r}-\mathbf{r}_0). \quad (2.4b)$$

Then, the original Green's function $G(\mathbf{r}|\mathbf{r}_0)$ is defined through the solution of the latter equation as

$$G(\mathbf{r}|\mathbf{r}_0) = \frac{i}{2k}\int_0^\infty d\tau \exp(ik\tau/2) g(\mathbf{r},\tau|\mathbf{r}_0,0). \quad (2.5)$$

Here, it is assumed that while ε is a real function, k contains an (infinitesimally small) positive imaginary part that enforces the radiation condition at infinity and provides the convergence of the corresponding integral. The generalized parabolic equation (2.4), being of exactly the same form as the standard equation used to describe the propagation of directed waves in a paraxial approximation, has a higher dimensionality than the latter. The difference of the problem associated with Eq. (2.5), from usual paraxial approximation, is that here all kinds of trajectories are allowed, including those with multiple turning points (backscattering), and passing many times through the same points (recurrent events).

The essential difficulty associated with representation (2.5) is that it contains an integral over pseudotime coordinate τ, with a rapidly oscillating integrand. In order to dispose of that integral while keeping the procedure to be physically correct, we derive a series expansion for the Green's function G. The main advantage of this expansion is that accounting for even the first term of this series allows one to describe consistently the statistical behavior of the wave propagating in strongly scattering media. Without loss of generality, we present the solution of Eq. (2.4) in a multiplicative form $g=g_0 g_\varepsilon$, where the first factor g_0 is the homogeneous medium Green's function, while the second factor g_ε accounts for the disorder. Then, we apply a formal procedure, presenting the inhomogeneous factor g_ε as

$$g_\varepsilon(\mathbf{r},\tau|\mathbf{r}_0,0) = \int_{-\infty}^\infty ds\, \delta(s-\tau) g_\varepsilon(\mathbf{r},s|\mathbf{r}_0,0). \quad (2.6)$$

Replacing now the δ function by its spectral expansion, and interchanging the integration order in Eq. (2.5), we arrive at

$$G(\mathbf{r}|\mathbf{r}_0) = \int_{-\infty}^\infty ds g_\varepsilon(\mathbf{r},s|\mathbf{r}_0,0)\frac{1}{2\pi}\int_{-\infty}^\infty d\Omega \times \exp[i(s-L)\Omega] F_m(\Omega), \quad (2.7)$$

where we have introduced the function

$$F_m(\Omega) = \int_0^\infty d\tau \exp(ik\tau/2 - i\tau\Omega) g_0(\mathbf{r},\tau|\mathbf{r}_0,0). \quad (2.8)$$

Evaluating the integral over τ in Eq. (2.8) leads to

$$F_m(\Omega) = (i/4)(k\sqrt{1-2\Omega/k}/2\pi L)^{m/2-1} \exp(iL\Omega) \times H^{(1)}_{m/2-1}(k\sqrt{1-2\Omega/k}L), \quad (2.9)$$

where $L=|\mathbf{r}-\mathbf{r}_0|$ is the distance between the source and the observation point and $H^{(1)}_{m/2-1}(\cdots)$ is the Hankel function. Actually, $F_m(\Omega)$ being multiplied by $\exp(-iL\Omega)$ can be identified with the free-space Green's function for the field with a rescaled wave number $\tilde{k}=k\sqrt{1-2\Omega/k}$. In Eq. (2.7), we may expand the function $F_m(\Omega)$ in a Taylor series in the neighborhood of the point $\Omega=0$, where the function is analytic. Then, the integrals over Ω give the derivatives of the δ function, and we obtain a series expansion for the unknown propagator

$$G(\mathbf{r}|\mathbf{r}_0) = \sum_{n=0}^\infty \frac{(-i)^n}{n!} F_m^{(n)}(0) g_\varepsilon^{(n)}(\mathbf{r},L|\mathbf{r}_0,0), \quad (2.10)$$

where the derivatives of g_ε with respect to the pseudotime are calculated at $\tau=L$. Since the function $F_m(\Omega)$ is analytic in the neighborhood of the point $\Omega=0$, the series expansion obtained has to be absolutely convergent.

In a statistical problem of wave propagation in random media, the calculation of the field itself is not necessary and the aim of the theory is to evaluate the statistical moments of the field such as mean (coherent) field or a second order coherence function. The main contribution to the statistical moments is provided by the zeroth-order term of the propagator expansion

$$G(\mathbf{r}|\mathbf{r}_0) \simeq G_0(\mathbf{r}|\mathbf{r}_0) g_\varepsilon(\mathbf{r},L|\mathbf{r}_0,0), \quad (2.11)$$

which actually reduces the problem to that of directed waves, though propagating in a higher-dimensional $(m+1)$ space with scattering potential that is uniform along the pseudotime axis. For instance, by using propagator (2.11) to evaluate the mean field, we reproduce the standard result of the diagrammatic approach, namely, the Bourret approximation, while higher order terms add only small corrections in the far field [15]. Also, applying the same propagator to the analysis of wave intensity behavior in a typical realization of the one-dimensional random media with correlated disorder, we obtain the well-known classical formula expressing the localization length through the power spectrum taken at the wave number of the resonant Bragg lattice [16,17].

III. COHERENCE FUNCTION

Using the approximate model of the propagator derived in the previous section, we consider now the two-frequency mutual coherence function

$$\Gamma(\omega,\Omega) = \langle G_{\omega+\Omega/2}(\mathbf{r}|\mathbf{r}_0) G^*_{\omega-\Omega/2}(\mathbf{r}|\mathbf{r}_0)\rangle, \quad (3.1)$$

where, to simplify the calculations, we assume that there is no separation between the points in both source and observation planes. Without any loss of generality we assume also that $\mathbf{r}_0=\mathbf{0}$. As follows from Eq. (2.11), the coherence function may be approximated by the corresponding solution obtained for a generalized directed wave propagating along the pseudotime coordinate τ in an artificially constructed medium with a m-dimensional transverse coordinate. This problem may be solved by resorting to a cumulant expansion of the corresponding path integral. This strategy has been very successful in our previous studies aimed at both evaluating the mean field [15] and exploring the strong localization phenomenon [16,17].

Using the so-called velocity (or white-noise) representation of the Feynman path integral [3], the Green's function g for a field with wave number k may be written as

$$g(\mathbf{r},\tau|\mathbf{r}_0,0) = \int D\mathbf{v}(t)\,\delta\left[\mathbf{r}-\mathbf{r}_0-\int_0^\tau dt\mathbf{v}(t)\right] \times\exp\left\{i\frac{k}{2}\int_0^\tau dt\left[\mathbf{v}^2(t)+\tilde{\varepsilon}\left(\mathbf{r}_0+\int_0^t dt'\mathbf{v}(t')\right)\right]\right\}, \tag{3.2a}$$

with the normalization condition

$$\int D\mathbf{v}(t)\exp\left[i\frac{k}{2}\int_0^\tau dt\mathbf{v}^2(t)\right]=1. \tag{3.2b}$$

To evaluate the coherence function, we first rescale the integration paths $\mathbf{v}_i(t)$ as $\mathbf{v}_i(t)\to\alpha_i\mathbf{v}_i(t)$, where the coefficients α_i are given by

$$\alpha_i\equiv\alpha_i(\omega,\Omega)=\sqrt{k(\omega)/k(\omega_i)},\quad i=1,2, \tag{3.3}$$

and $k\equiv k(\omega)$ is the wave number corresponding to a "central" frequency ω. Then, introducing the Wigner type functional variables

$$\mathbf{w}(t)=\frac{1}{2}[\mathbf{v}_1(t)+\mathbf{v}_2(t)],\quad \mathbf{v}(t)=\mathbf{v}_1(t)-\mathbf{v}_2(t), \tag{3.4}$$

and performing ensemble averaging, we arrive at

$$\Gamma(\omega,\Omega)=\Gamma_0(\omega,\Omega)\eta^m\int D\mathbf{w}(t)\int D\mathbf{v}(t) \times\delta\left[\alpha\eta\mathbf{r}-\int_0^L dt\mathbf{w}(t)\right]\delta\left[\beta\eta\mathbf{r}+\int_0^L dt\mathbf{v}(t)\right] \times\exp\left[ik\int_0^L dt\mathbf{w}(t)\cdot\mathbf{v}(t)\right] \times\exp\{-X[\mathbf{w}(t),\mathbf{v}(t);\omega,\Omega]\}, \tag{3.5}$$

where $\Gamma_0(\omega,\Omega)$ is the coherence function in a homogeneous reference medium, the functional X has the form

$$X[\mathbf{w}(t),\mathbf{v}(t);\omega,\Omega] =\frac{k^2}{8}\int_0^L dt_1\int_0^L dt_2\{\eta_1^2B_\varepsilon[\mathbf{r}_1(t_1)-\mathbf{r}_1(t_2),\omega_1,0] -2\eta^2B_\varepsilon[\mathbf{r}_1(t_1)-\mathbf{r}_2(t_2),\omega,\Omega] +\eta_2^2B_\varepsilon[\mathbf{r}_2(t_1)-\mathbf{r}_2(t_2),\omega_2,0]\} \tag{3.6}$$

and a number of dimensionless coefficients are defined as follows:

$$\alpha=(\alpha_1+\alpha_2)/2,\quad \beta=\alpha_1-\alpha_2, \tag{3.7a}$$

$$\eta_1=1/\alpha_1^2,\quad \eta=1/(\alpha_1\alpha_2),\quad \eta_2=1/\alpha_2^2, \tag{3.7b}$$

each one depending on the frequency shift Ω. Note that additional arguments in the correlation functions $B_\varepsilon(\cdots)$ take into account an arbitrary permittivity dispersion. The functional paths $\mathbf{r}_1(t)$ and $\mathbf{r}_2(t)$, entering Eq. (3.6) are, in their turn, given by

$$\mathbf{r}_1(t)=\alpha_1\int_0^t dt[\mathbf{w}(t)+\mathbf{v}(t)/2], \tag{3.8a}$$

$$\mathbf{r}_2(t)=\alpha_2\int_0^t dt[\mathbf{w}(t)-\mathbf{v}(t)/2]. \tag{3.8b}$$

To evaluate the path integral in Eq. (3.5), we use a perturbative technique in which the expectation value of the exponential $\exp(-X)$ over all possible paths is replaced by the exponent of a (truncated) series over corresponding cumulants, $\chi(\omega,\Omega)$, such that the coherence function is expressed as

$$\Gamma(\omega,\Omega)=\Gamma_0(\omega,\Omega)\exp[-\chi(\omega,\Omega)]. \tag{3.9}$$

Actually, the path integral can be evaluated perturbatively not only for the functional $X(\omega,\Omega)$ itself, but also for its (implicitly assumed much smaller) deviation from $X(\omega,0)$. Indeed, the path integral in Eq. (3.5) may be split approximately as

$$\int\exp[-X(\omega,\Omega)]\simeq\int\exp[-X(\omega,0)]\int\exp[-\tilde{X}(\omega,\Omega)], \tag{3.10}$$

where

$$\tilde{X}(\omega,\Omega)=X(\omega,\Omega)-X(\omega,0), \tag{3.11}$$

and the integral sign abbreviates the expectation over a set of "velocities" $\mathbf{w}(t)$ and $\mathbf{v}(t)$. This splitting of the path integral is by virtue of the fact that the two functionals $X(\omega,0)$ and $\tilde{X}(\omega,\Omega)$ are practically uncorrelated in the function space, as can be verified by direct numerical simulations of the white-noise trajectories. As a result, the normalized correlator

$$\tilde{\Gamma}(\omega,\Omega)=\Gamma(\omega,\Omega)/\Gamma(\omega,0)=\tilde{\Gamma}_0(\omega,\Omega)\exp[-\tilde{\chi}(\omega,\Omega)], \tag{3.12}$$

even though based on calculating the first cumulant alone, should be rather accurate in a much broader scattering framework than the same approximation for the mean intensity is.

We begin here by performing the calculations for the functional $X(\omega,\Omega)$ in its original form, while the normalization will be carried out in Sec. V. The first cumulant (linear with respect to the correlation function) is calculated by firstly replacing the correlation functions in Eq. (3.6) with their spectral expansions. This allows us to present the coherence function, at least for dispersionless media, as an integral transform of the power spectrum

$$\chi(\omega,\Omega)=\frac{\pi}{2}k^3L\int d\mathbf{K}f(\mathbf{K},\omega,\Omega)\Phi_\varepsilon(\mathbf{K}), \tag{3.13}$$

with a kernel $f(\mathbf{K},\omega,\Omega)$ called the filtering function in the sequel. This function consists of three terms as follows:

$$f(\mathbf{K},\omega,\Omega)=\eta_1^2f_{11}(\mathbf{K},\omega,\Omega)-2\eta^2f_{12}(\mathbf{K},\omega,\Omega) +\eta_2^2f_{22}(\mathbf{K},\omega,\Omega), \tag{3.14}$$

where

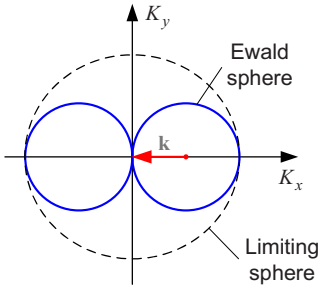

FIG. 1. (Color online) Ewald diagram (two-dimensional case is shown). The points of the Ewald sphere for a given wave vector **k** determine all possible spectral components **K** that could resonantly transform the incident wave into a scattered one. The limiting sphere encircles all spectral components coupling any two wave vectors in the process of elastic scattering.

$$f_{ij}(\mathbf{K},\omega,\Omega) = (4\pi kL)^{-1}\eta^m \int_0^L dt_1 \int_0^L dt_2 \int D\mathbf{w}(t) \int D\mathbf{v}(t) \times \delta\left[\alpha\eta\mathbf{r} - \int_0^L dt\mathbf{w}(t)\right]\delta\left[\beta\eta\mathbf{r} + \int_0^L dt\mathbf{v}(t)\right] \times \exp\left[ik\int_0^L dt\mathbf{w}(t)\cdot\mathbf{v}(t)\right] \times \exp\{i\mathbf{K}\cdot[\mathbf{r}_i(t_1) - \mathbf{r}_j(t_2)]\}. \quad (3.15)$$

As is shown in Appendix A, in the far field this weighting factor has the form

$$f(\mathbf{K},\omega,\Omega) = K^{-1}\frac{2}{\pi}\int_0^\infty dx\,\cos(2x\mathbf{k}\cdot\mathbf{K}/K)[\cos(xK) - \mathrm{sinc}(xK)\exp(i\Omega LK^2/8ck^2 - i\Omega L\mathbf{K}\cdot\mathbf{k}/4ck^2)], \quad (3.16)$$

where c is the wave velocity in a homogeneous reference medium. In terms of generalized functions the latter expression becomes

$$f(\mathbf{K},\omega,\Omega) = K^{-1}\delta(K - |2\mathbf{k}\cdot\mathbf{K}/K|) - K^{-2}\exp[i\Omega L(K/8ck^2)(K - 2\mathbf{k}\cdot\mathbf{K}/K)] \times \vartheta(K - |2\mathbf{k}\cdot\mathbf{K}/K|), \quad (3.17)$$

where, as previously, $\delta(\cdots)$ is the Dirac δ function and $\vartheta(\cdots)$ is the Heaviside step function. The filtering function can be mapped onto the Ewald diagram (see Fig. 1), which is a very useful tool in analyzing, e.g., the x-ray diffraction by crystals [23] and also in diffraction tomography [24]. As follows from Eq. (3.17), the loss of coherence between two waves with different frequencies is due to both Bragg scattering on spectral components lying within the limiting sphere of the Ewald diagram ($K \leqslant 2k$) and to local high-frequency resonances ($K > 2k$).

Another issue that can be covered by using the result obtained is the role of dissipation. In an absorptive medium, the dissipation is usually accounted for by taking the scattering potential (permittivity or refractive index) to be a complex-valued field. When the dissipation is small, a possible alternative is to consider the scattering potential to be real while assigning a small imaginary part to the frequency, i.e., transforming the wave number as $k \to k + i\gamma$, where γ is the decrement of the field. Note that just the latter approach makes the corresponding integral in Eq. (2.5) convergent. Thus, in a homogeneous absorptive medium, the intensity of the wave will decrease as $\exp(-L/l_a)$, the factor that has to be included in the expression for $\Gamma_0(\omega,\Omega)$. Obviously, the absorption length l_a is given by $l_a = 1/2\gamma$. Since the two frequencies are defined now as

$$\omega_1 \simeq \omega + ic\gamma + \Omega/2, \quad \omega_2^* \simeq \omega - ic\gamma - \Omega/2, \quad (3.18)$$

we could include the absorption by substituting $\Omega \to \Omega + 2ic\gamma$ in the filtering function.

For a given spectrum $\Phi_\varepsilon(\mathbf{K})$, the final result depends on both the modulus and direction of the wave vector **k**. Here we will concentrate on the analysis of wave propagation in isotropic three-dimensional media, where a diffusionlike spread of the wave energy in the time domain takes place. Therefore, for isotropic spectra $\Phi_\varepsilon(K)$ we can integrate in Eq. (3.13) over angular variables, which results in

$$\chi(\omega,\Omega) = \pi^2 k^2 L \int_0^\infty dK K f(K,\omega,\Omega)\Phi_\varepsilon(K). \quad (3.19)$$

For convenience, we extracted the general factor $1/kK$ from the filtering function, the latter after integration takes the form (see Appendix B)

$$f(K,\omega,\Omega) = [1 - \exp(i\Omega LK^2/8ck^2)\mathrm{sinc}(\Omega LK^2/8ck^2)] \times \vartheta(2k - K) - (2k/K)\exp(i\Omega LK^2/8ck^2) \times \mathrm{sinc}(\Omega LK/4ck)\,\vartheta(K - 2k). \quad (3.20)$$

It is instructive now to compare the high-frequency limit of the result obtained to that of directed waves (i.e., by assuming the propagation in a large-scale weakly scattering random medium). In principle, the approximations we have used do not allow us to extend the final result to directed waves. In fact, for directed waves the relevant vectors **K** are much smaller in size than the wave number k, so the integration is performed over a very small region near the origin of the Fourier space. Moreover, as follows from the geometry of the directed wave propagation and is seen by inspecting the Ewald diagram, Fig. 1, scalar product $2\mathbf{k}\cdot\mathbf{K}$ vanishes in this case, violating the necessary conditions imposed on the corresponding parameters on the way to final results (see Appendix A). Nevertheless, our approximation does make sense even in the ballistic regime. Indeed, for the directed waves, the ratio $K/2k$ is so small that we can neglect totally the contribution of the high-frequency tail ($K > 2k$) in Eq. (3.20). Comparing the resulting expression for the filtering function with a corresponding linearized solution obtained for directed waves [7]

$$f(K,\omega,\Omega) = 1 - \exp(i\Omega LK^2/8ck^2) \times {}_1F_1(1/2,3/2;-i\Omega LK^2/8ck^2), \quad (3.21)$$

where ${}_1F_1(a,b;z)$ is the hypergeometric Kummer function,

we see that they look similar, although Eq. (3.21) predicts approximately two times faster loss of coherence then our extrapolated result does.

Also, since no limitations have been imposed on the coherence function for wave propagation in media with small-scale disorder, we can conclude that the result obtained should be valid in a rather wide range of wavelengths, including the most interesting resonant regime where the wavelength is of the same order as the correlation scale of the disorder and, therefore, the coherent effects should be especially pronounced [8].

IV. WAVE TRANSPORT IN THE TIME DOMAIN

Our ultimate goal here is to evaluate the normalized correlator $\tilde{\Gamma}(\omega,\Omega)$. Indeed, for a very short (but still narrowband) wave packet, such as a picosecond pulse of visible light, $\tilde{\Gamma}(\omega,\Omega)$ and the normalized impulse response function (photon time of flight distribution) $J(\omega,t)$ constitute a Fourier transform pair [1]

$$J(\omega,t) = \frac{1}{2\pi}\int_{-\infty}^{\infty} d\Omega \exp(-i\Omega t)\tilde{\Gamma}(\omega,\Omega). \tag{4.1}$$

By considering Eq. (3.13), we see that our approach describes photon migration as a process of subsequent scattering of the wave by resonant Bragg lattices of all possible directions and periods hidden in a disordered structure, and takes into account an additional dwell time due to the local resonances. This resembles a usual random walk in the time domain but accounts for the wave interference effects and for the wave energy accumulation inside resonant clusters. Moreover, the shape of the pulse, which can be reconstructed using Eq. (4.1), is related to actual correlation properties of the scattering medium, rather than to a phenomenological diffusion constant.

For large distances, the behavior of the cumulant $\tilde{\chi}(\omega,\Omega)$ is determined by small values of Ω. Formally, we can expand the filtering function in a series, which leads to

$$\tilde{\chi}(\omega,\Omega) = \tilde{\chi}'(\omega,0)\Omega + \tilde{\chi}''(\omega,0)\Omega^2/2 + \cdots, \tag{4.2}$$

where, as can be shown [7], the linear term is related to the delay time $\tilde{\tau}=i\partial_\Omega\tilde{\chi}(\omega,0)$, while the quadratic term corresponds to a pulse width squared $\tilde{w}^2=\partial_\Omega^2\tilde{\chi}(\omega,0)$.

Differentiating Eq. (3.19) for lossless media, we arrive at

$$\tilde{\tau} = \pi^2 k^3 L^2 c^{-1}\int_0^{\infty} dK f_\tau(K)\Phi_\varepsilon(K), \tag{4.3}$$

where the filtering function $f_\tau(K)$ has the form

$$f_\tau(K) = (K/2k)^3\vartheta(2k-K) + (K/2k)^2\vartheta(K-2k). \tag{4.4}$$

For large-scale inhomogeneities, only the first term in the latter expression should be retained, that leads to a frequency-independent delay time $\tilde{\tau}$, a natural result in the framework of geometric optics. In the opposite regime, the delay time increases linearly as a function of k.

Analogous calculations for the pulse width $\tilde{w}$ result in

$$\tilde{w}^2 = \frac{2}{3}\pi^2 k^3 L^3 c^{-2}\int_0^{\infty} dK f_w(K)\Phi_\varepsilon(K), \tag{4.5}$$

where

$$f_w(K) = (K/2k)^5\vartheta(2k-K) + \frac{1}{4}(K/2k)^2[1+3(K/2k)^2] \times\vartheta(K-2k). \tag{4.6}$$

As follows from Eq. (4.5), $\tilde{w}$ decreases with frequency in the geometric optics regime. For low frequencies, however, the pulse width diverges as $k^{-1/2}$. This asymptotic behavior is related to a very long tail typical of the mean intensity in this regime due to slow damping of the local high-Q resonances in lossless media.

The higher order terms of the series expansion (4.2) specify the asymmetry and other fine details of the pulse shape. For $L\to\infty$ and sufficiently large values of k, the higher order terms may be neglected, which leads, after completing Fourier transform (4.1), to a symmetric Gaussian form of the impulse response function $J(t)$. Obviously, such asymptotic behavior contradicts the classical time domain behavior of a short pulse in the diffusion limit, and should be attributed to the limitations of our model based on the first cumulant. However, as we will see later on, our results are consistent with known experimental data in the intermediate regime of moderately strong scattering where both ballistic and diffuse components of the wave may be equally important. Despite the fact that the higher cumulants are significant for evaluating the coherence function or the impulse response in the diffuse regime, their contribution to the delay time [first derivative of $\tilde{\chi}(\omega,\Omega)$ taken at $\Omega=0$] is exactly zero whatever strong the disorder is, and our estimate of $\tilde{\tau}$ should remain viable even when the accuracy in evaluating $\tilde{\Gamma}(\omega,\Omega)$ is lost.

V. EXAMPLES

In order to exemplify the results we start with the Gaussian correlation function of the form

$$B_\varepsilon(r) = \sigma_\varepsilon^2 \exp(-r^2/l_\varepsilon^2), \tag{5.1}$$

where σ_ε^2 and l_ε characterize, respectively, the strength and correlation scale of the disorder. In 3D case this corresponds to the power spectrum

$$\Phi_\varepsilon(K) = (2\sqrt{\pi})^{-3}\sigma_\varepsilon^2 l_\varepsilon^3 \exp(-l_\varepsilon^2 K^2/4). \tag{5.2}$$

Although the Gaussian function is not related directly to a specific physical mechanism responsible for the heterogeneous medium formation, and even cannot correspond to any two-phase random medium [25], it is an effective mathematical model widely used to characterize the wave propagation in a broad class of random media having a single correlation scale (in contrast, for example, with fractal media where $\Phi_\varepsilon(K)$ has a power law decay), when the exact form of $B_\varepsilon(r)$ is not known or in order to perform a qualitative analysis [1].

For this model, the normalized cumulant $\tilde{\chi}(\omega,\Omega) = \chi(\omega,\Omega)-\chi(\omega,0)$ entering Eq. (3.12) becomes

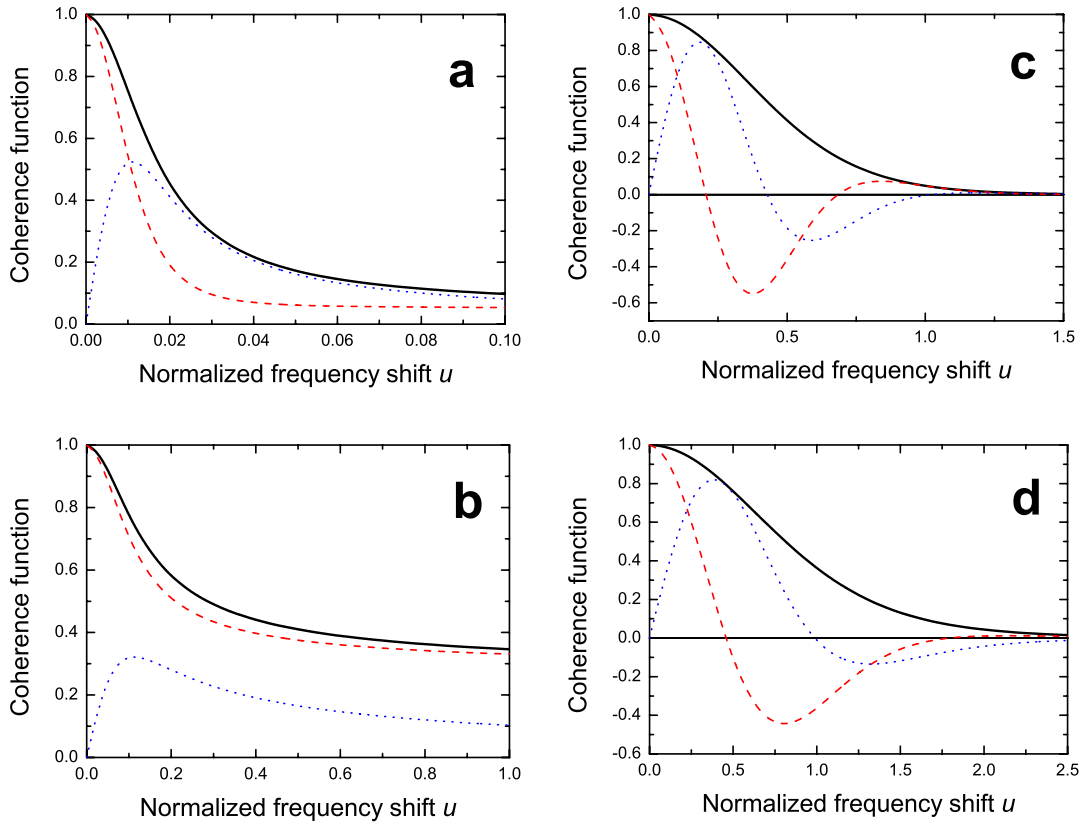

FIG. 2. (Color online) Normalized coherence function $\tilde{\Gamma}(\omega,\Omega)$ plotted for $L/l_s=20$ and different values of the normalized wave number and absorption length: (a) $\kappa=0.1$, $\upsilon=0.0$; (b) $\kappa=0.1$, $\upsilon=0.05$; (c) $\kappa=1.0$, $\upsilon=0.0$; (d) $\kappa=1.0$, $\upsilon=1.0$. The absolute value of $\tilde{\Gamma}(\omega,\Omega)$ is shown by solid line, while dashed and dotted lines correspond, respectively, to the real and imaginary parts of the coherence function.

$$\tilde{\chi}(\kappa,u)=s(\kappa,u)L/l_s, \tag{5.3}$$

where l_s, given by

$$l_s^{-1}=\frac{\sqrt{\pi}}{4}k^2 l_\varepsilon \sigma_\varepsilon^2, \tag{5.4}$$

is the first-order approximation for the scattering mean-free path [15]. The factor $s(\kappa,u)$ being a function of two parameters, specifically, the normalized wave number $\kappa=kl_\varepsilon$ and the normalized frequency shift $u=\Omega L/c$ can be presented as a sum of two terms

$$s(\kappa,u)=s_{\mathrm{LF}}(\kappa,u)+s_{\mathrm{HF}}(\kappa,u). \tag{5.5}$$

The first, low-frequency ($K\leqslant 2k$), term reads

$$s_{\mathrm{LF}}(\kappa,u)=1-\exp(-\kappa^2)-i(\kappa^2/u)\times[\ln(1-iu/\kappa^2)+E_1(\kappa^2-iu)-E_1(\kappa^2)], \tag{5.6}$$

where $E_1(z)$ is the exponential integral. The second, high-frequency ($K>2k$), term is of the form

$$s_{\mathrm{HF}}(\kappa,u)=\sqrt{\pi}\kappa\,\mathrm{erfc}(\kappa)-2\pi(\kappa^2/u)\mathrm{erf}(u/4\sqrt{\kappa^2-iu/2})+2\kappa^2 W_{u/2}(\kappa^2-iu/2), \tag{5.7}$$

where $\mathrm{erf}(\cdots)$ and $\mathrm{erfc}(\cdots)$ are the error and complementary error functions, respectively, and $W_\alpha(\cdots)$ is given by a rapidly converging (for $\kappa\leqslant 1$) series

$$W_\alpha(z)=\sum_{n=0}^{\infty}\sum_{k=0}^{n}\frac{(-1)^n\alpha^{2(n-k)}(2z)^k}{(2n+1)(2n+1-2k)!(2k)!!}. \tag{5.8}$$

Calculations show that for the value of κ greater than 2–3 we can neglect the contribution of the high-frequency term. For lossy media, the frequency shift u becomes complex valued: $u\to u+iv$, where $v=L/l_a$ is the normalized absorption coefficient.

Figures 2 show some examples of the normalized coherence function evaluated for $L/l_s=20$ and different values of κ and v. It is seen that for relatively low frequencies ($\kappa=0.1$), the coherence function has a two-scale structure, with a rather quick decay at small frequency shifts u and a long tail for larger values of u. For instance, the value of $|\Gamma|$ calculated for the wave propagating in a lossless scattering medium, decreases rather quickly down to the value of 0.1 already for $u\sim 0.1$, but remains practically unchanged at the same level up to $u\sim 15$. Being transformed to the time domain, these two scales can be attributed, correspondingly, to diffuse and ballistic components, coexisting even in the strong scattering regime. The bimodal structure of the photon time-of-flight distribution has been described previously in a number of publications, all based on a time domain version of the radiative transfer equation [26,27]. Our model is the

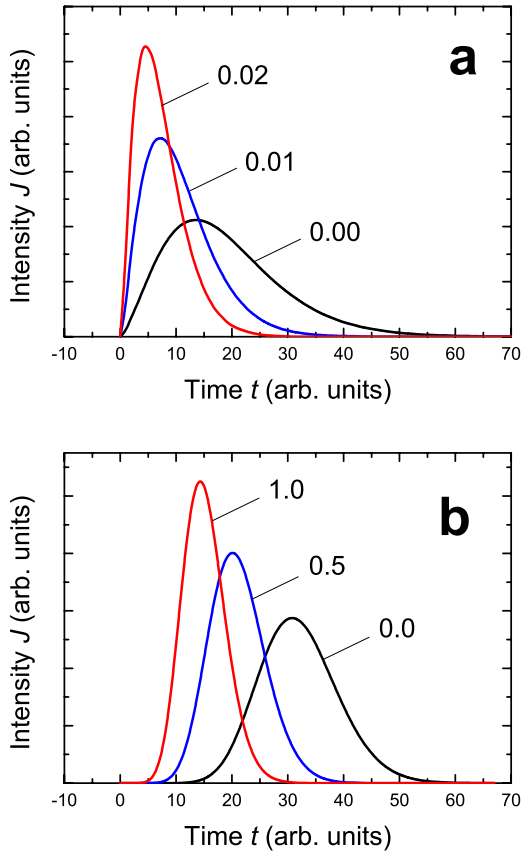

FIG. 3. (Color online) Profiles of the mean intensity $J(t)$ deep in the diffusion regime ($L/l_s=50$) calculated for different values of the normalized wave number: (a) $\kappa=0.1$; (b) $\kappa=1.0$. Time scales are different for the two plots. In both cases, the increase in absorption corresponds to shorter intensity profiles with higher maxima.

first, to our knowledge, that predicts this effect and at the same time has been derived directly from the wave equation. Note that the possibility of separate observation of ballistic photons constitutes a physical basis for the time gating technique improving essentially spatial resolution in near-infrared spectroscopy [19].

In the diffusion regime ($L/l_s \gg 1$), the results of the calculations are also consistent, at least qualitatively, with known experimental data [28–30]. The absorption enhances essentially the coherence (attention should be paid to the difference in the frequency scale between corresponding plots in Fig. 2), which is quite clear from the physical point of view, because the long paths are eliminated in this case. For higher frequencies, the effect of absorption is much less pronounced, that can be explained by a decrease of the wave energy accumulated inside resonant clusters in this regime. A number of examples for the mean intensity profiles in the diffusion regime are shown in Fig. 3. As can be seen, the increase of absorption leads to shorter impulse response and smaller delay time.

The first temporal moments of the mean intensity for the Gaussian model can be presented in an analytical form. In particular, the delay time $\tilde{\tau}$ given by Eq. (4.3) in the absence of absorption is written as

$$\tilde{\tau} = \frac{\sqrt{\pi}}{8}\left(1 - e^{-\kappa^2} + \frac{\sqrt{\pi}}{2}\kappa \operatorname{erfc} \kappa\right)\sigma_\varepsilon^2 L^2/cl_\varepsilon. \qquad (5.9)$$

Although we have performed all the calculations for an infinite absorptionless media, it is instructive to compare this result with known experimental data obtained for finite samples. It makes sense because the effective geometry of the problem we solve here is rather similar to a finite length slab due to suppressing the contribution of scattering from the areas located far enough from both the source and the observation point. In a slab geometry, the diffusion theory approximates the delay time by $\tilde{\tau} \simeq L^2/6D$, where D is the diffusion constant [31]. Note that the same asymptotic behavior (although with a different coefficient) has also been predicted for the time-dependent radiative transfer equation with an impulsive point source located in an infinite medium [26]. Inasmuch as Eq. (5.9) reproduces correctly the L^2 dependence of the delay time, which is observed also in experiments, we could estimate the diffusion constant by connecting it to the microstructure of a specified random medium. We have tested the calculated values of the diffusion constant against the results of the measurements performed for ultrasound [28], microwaves [29], and optical waves [30], see the details summarized in Table I. Taking, rather arbitrarily, l_ε to be equal to the particle diameter, and setting $\sigma_\varepsilon \sim 1$ (high contrast media), we obtain the diffusion constant estimate of the same order of magnitude as the measured values of D. This fact is especially surprising since in all these experiments the radiation is of a vector nature, in contrast to the scalar model adopted here.

TABLE I. Diffusion constant (theoretical estimates calculated according to the relation $D \simeq L^2/6\tilde{\tau}$ and Eq. (5.9), vs. a number of experimentally measured values reported in the literature).

Parameters	Ultrasound [28]	Microwaves [29]	Optics [30]
Random system composition	glass beads in water[a] (impedance ratio 10)	polystyrene spheres ($n \sim 1.6$) in air	rutile TiO_2 particles ($n \sim 2.8$) in air
Diameter of particles	~0.5 mm	0.5 inch	150–290 nm
Volume filling factor	0.63	0.52	not available
Frequency	2.5 MHz	16.8–17.8 GHz	387 THz
Measured value of D	0.4 m^2/s	3.3×10^6 m^2/s	25 m^2/s
Estimate of D	1 m^2/s	2×10^6 m^2/s	20 m^2/s

[a]Sound velocity in water is approximately 1.5 km/s, while the longitudinal and transverse velocities of sound in glass are 5.7 and 3.4 km/s, respectively [28].

Both coherence function and impulse response are rather sensitive to the form of the correlation function $B_\varepsilon(r)$. Here we confine the calculations to the delay time for the exponential model

$$B_\varepsilon(r) = \sigma_\varepsilon^2 \exp(-r/l_\varepsilon), \tag{5.10}$$

first proposed by Debye and co-workers who believed that it should correspond to structures in which one phase consists of "random shapes and sizes," see Ref. [25]. In this case, the power spectrum takes the form

$$\Phi_\varepsilon(K) = \frac{\sigma_\varepsilon^2 l_\varepsilon^3}{\pi^2}(1 + K^2 l_\varepsilon^2)^{-2} \tag{5.11}$$

and decreases as K^{-4} for large wave numbers (a kind of fractal behavior) reflecting the fact that, at least theoretically, whatever small features can be found in any realization of the scattering medium. Substituting this spectrum into Eq. (4.3) leads to

$$\tilde{\tau} = \{\ln(1 + 4\kappa^2) + 2\kappa[\pi/2 - \arctan(2\kappa)]\}\sigma_\varepsilon^2 L^2/16cl_\varepsilon. \tag{5.12}$$

Thus, in the high-frequency limit the delay time grows logarithmically as a function of κ, in contrast to single-scale correlation functions such as the Gaussian model demonstrating a saturation in this regime.

VI. SUMMARY

In this work, the crossover from the ballistic to diffusive regime of wave propagation has been studied in the framework of a universal model, valid for random media of any dimensionality. The analytical results describing spectral coherence and time-domain transport of wave fields in random media, were obtained from first principles, without any resort to the radiative transfer equation, or its derivative, the diffusion model.

For rather large distances, the predictions of our theory are consistent with a classical diffusion paradigm and experimental data available in the literature. Although deep in the diffusion regime, our model is not accurate enough since the higher temporal moments are not reproduced correctly, the first two moments (namely, the delay time and the pulse width) are sufficiently viable. In particular, the delay time evaluated analytically is in a good agreement with the results of known measurements even for very strongly scattering media. This allows for the diffusion constant to be related directly to the statistics of the disorder. Moreover, it can be shown that the integral transform relating the delay time to the power spectrum is invertible, which allows one, in principle, to reconstruct the correlation function of a heterogeneous medium by measuring the angular distributions of the diffuse time for waves of different frequencies [32].

A similar analysis of spectral correlation and pulse evolution can be performed also for two-dimensional media. Since the coherence function has been expressed via the power spectrum of arbitrary form, the results obtained in the work open a new avenue in studying wave transport in anisotropic and/or fractally correlated systems.

ACKNOWLEDGMENTS

This work has been supported, in part, by the Office of Naval Research, under Grant No. N00014-00-1-0672.

APPENDIX A

The simplest trick for the effective evaluation of the path integral in Eq. (3.15) is to present the last exponential factor entering this equation in the form [7]

$$\exp\{i\mathbf{K}\cdot[\mathbf{r}_i(t_1) - \mathbf{r}_j(t_2)]\} = \exp\left[ik\int_0^L dt\mathbf{w}(t)\cdot\boldsymbol{\upsilon}_{ij}(t)\right] \times \exp\{i\mathbf{K}\cdot[\tilde{\mathbf{r}}_i(t_1) - \tilde{\mathbf{r}}_j(t_2)]\}, \tag{A1}$$

where

$$\boldsymbol{\upsilon}_{ij}(t) = [\alpha_i\vartheta(t_1 - t) - \alpha_j\vartheta(t_2 - t)]\mathbf{K}/k, \tag{A2}$$

$\vartheta(z)$ is the Heaviside step function, and the paths $\tilde{\mathbf{r}}(t)$ are obtained by dropping the $\mathbf{w}(t)$ term in Eqs. (3.8). As can be easily verified, this is just an identical transformation. In Eq. (3.15) we then replace the δ function containing $\mathbf{w}(z)$ by its spectral expansion and, using the definition of the δ functional [3],

$$\delta[\mathbf{v}(t)] = \int D\mathbf{w}(t)\exp\left[ik\int_0^L dt\mathbf{w}(t)\cdot\mathbf{v}(t)\right], \tag{A3}$$

perform sequentially the path integration over $\mathbf{w}(z)$ and $\mathbf{v}(z)$. As a result, neglecting the small term proportional to $\beta\mathbf{r}$ in the exponent, we arrive at

$$f_{ij}(\mathbf{K},\omega,\Omega) = (4\pi kL)^{-1}\int_0^L dt_1\int_0^L dt_2 \times\exp[i\alpha\eta(\alpha_i t_1 - \alpha_j t_2)\mathbf{K}\cdot\mathbf{r}/L] \times\exp[-i\sigma_{ij}(t_1,t_2)K^2/2k], \tag{A4}$$

where the functions σ_{ij} have the form

$$\sigma_{ii}(t_1,t_2) = (-1)^{i-1}\alpha_i^2[t_1(1 - t_1/L) + t_2(1 - t_2/L) - 2\min(t_1,t_2) + 2t_1t_2/L], \tag{A5a}$$

$$\sigma_{12}(t_1,t_2) = \alpha_1^2 t_1(1 - t_1/L) - \alpha_2^2 t_2(1 - t_2/L). \tag{A5b}$$

To simplify the expressions for the filtering functions f_{11} and f_{22}, we introduce a new pair of integration variables

$$t = (t_1 + t_2)/2, \quad \tau = t_1 - t_2. \tag{A6}$$

Then, the integration domain in the (t,τ) plane represents a rhombus confined by the lines $t = \pm\tau/2$ and $t = L \pm \tau/2$, see Fig. 4(a). Since the functions $\sigma_{ii}(t_1,t_2)$ are converted into

$$\sigma_{ii}(\tau) = (-1)^{i-1}\alpha_i^2|\tau|(1 - |\tau|/L) \tag{A7}$$

and, therefore, the integrands turn out to be independent of t, the integration becomes trivial and we have

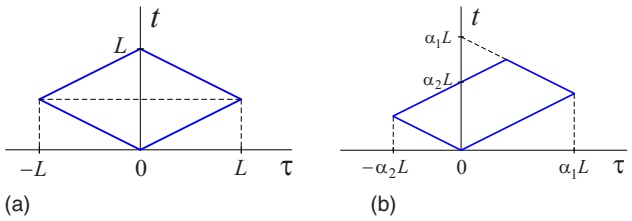

FIG. 4. (Color online) (a) Integration domain for evaluating the filtering functions f_{11} and f_{22}. (b) Integration domain for evaluating the filtering function f_{12}.

$$f_{ii}(K,\omega,\Omega) = (2\pi k)^{-1}\int_0^L d\tau(1-\tau/L)\cos[(\alpha\alpha_i/\alpha_1\alpha_2)\tau\mathbf{K}\cdot\mathbf{r}/L] \times \exp[(-1)^i i\alpha_i^2\tau(1-\tau/L)K^2/2k]. \quad \text{(A8)}$$

The evaluation of the filtering function f_{12} is a bit more intricate. In order to obtain a linear dependence on t in the exponent, we first rescale the integration variables as $\alpha_1 t_1 \to t_1$ and $\alpha_2 t_2 \to t_2$, and only after that introduce the pair (t,τ) defined by Eqs. (A6). Then, the filtering function f_{12} reduces to the form

$$f_{12}(\mathbf{K},\omega,\Omega) = (4\pi kL)^{-1}\eta\int\int_{\Re} dtd\tau\exp(i\alpha\eta\tau\mathbf{K}\cdot\mathbf{r}/L) \times \exp[-i(\alpha\tau+\beta t-2\tau t/L)K^2/2k], \quad \text{(A9)}$$

where the integration domain $\Re$ in the (t,τ) plane is a parallelogram confined by the lines $t=\pm\tau/2$, $t=\alpha_1 L-\tau/2$, and $t=\alpha_2 L+\tau/2$, see Fig. 4(b). For an arbitrary function $\varphi(t,\tau)$, this parallelogram can be decomposed into three triangles as

$$\int\int_{\Re} dtd\tau\varphi(t,\tau) = \int_0^{\alpha_1 L} d\tau\int_{\pi/2}^{\alpha_1 L-\tau/2} dt\varphi(t,\tau) + \int_0^{\alpha_2 L} d\tau\int_{\pi/2}^{\alpha_2 L-\tau/2} dt\varphi(t,-\tau) - \int_0^{\beta L} d\tau\int_{\alpha_2 L+\tau/2}^{\alpha_1 L-\tau/2} dt\varphi(t,\tau). \quad \text{(A10)}$$

Evaluating the corresponding integrals over t leads to

$$f_{12}(\mathbf{K},\omega,\Omega) = (4\pi k)^{-1}\eta\left[\alpha\int_0^{\alpha_1 L} d\tau(1-x_1/L)\exp(i\alpha\eta\tau\mathbf{K}\cdot\mathbf{r}/L)S_\alpha(x_1) + \alpha\int_0^{\alpha_2 L} d\tau(1-x_2/L)\exp(-i\alpha\eta\tau\mathbf{K}\cdot\mathbf{r}/L)S_\alpha(x_2) - (\beta/2)\int_0^{\beta L} d\tau(1-x_3/L)\exp(i\alpha\eta\tau\mathbf{K}\cdot\mathbf{r}/L)S_{\beta/2}(x_3)\right], \quad \text{(A11)}$$

where

$$x_1 = \alpha\tau+\beta L/2, \quad x_2 = \alpha\tau-\beta L/2, \quad x_3 = \beta\tau/2+\beta L/2, \quad \text{(A12)}$$

and

$$S_q(x) = \exp[-i\nu L(1-x/L)K^2/4k]\mathrm{sinc}[q^2 x(1-x/L)K^2/2k]. \quad \text{(A13)}$$

Hereafter, we denote $\nu=\alpha\beta$ and $\mathrm{sinc}(x)=\sin(x)/x$. Now, appropriately changing the integration variables, we find

$$f_{12}(\mathbf{K},\omega,\Omega) = (4\pi k)^{-1}\eta\exp(i\nu\eta\mathbf{K}\cdot\mathbf{r}/2)\left[\alpha^2\int_{-\beta L/2\alpha}^{L} d\tau(1-\tau/L)\exp(i\alpha^2\eta\tau\mathbf{K}\cdot\mathbf{r}/L)S_\alpha(\tau) + \alpha^2\int_{\beta L/2\alpha}^{L} d\tau(1-\tau/L)\exp(-i\alpha^2\eta\tau\mathbf{K}\cdot\mathbf{r}/L)S_\alpha(\tau) - (\beta/2)^2\int_{-L}^{L} d\tau(1-\tau/L)\exp(i\nu\eta\tau\mathbf{K}\cdot\mathbf{r}/2L)S_{\beta/2}(\tau)\right]. \quad \text{(A14)}$$

Substituting formulas (A8) and (A14) for the filtering functions f_{ij} into Eqs. (3.14) and then (3.13), we obtain a general expression for the cumulant $\chi(\omega,\Omega)$, valid for arbitrary frequency shift and receiver location. Further simplification could be performed if we assume that the normalized frequency shift ν is rather small, while the path length L and the value of vector $\mathbf{r}=L\mathbf{k}/k$ are large (to simplify the notation, we assign the direction of $\mathbf{r}$ to the wave vector $\mathbf{k}$). Then, it is reasonable to keep the dependence on frequency shift ν only in combination νL, and to neglect simultaneously the dependence on ν by putting $\alpha_1=\alpha_2=1$ in all other cases. Taking into account also that $\nu=-\Omega/2ck\eta^2$, we arrive at

$$f(\mathbf{K},\omega,\Omega) = (\pi k)^{-1}\int_0^L d\tau(1-\tau/L)\cos(\tau\mathbf{K}\cdot\mathbf{k}/k) \times\{\cos[\tau(1-\tau/L)K^2/2k] - \mathrm{sinc}[\tau(1-\tau/L)K^2/2k] \times\exp[i\Omega L(1-\tau/L)K^2/8ck^2 - i\Omega L\mathbf{K}\cdot\mathbf{k}/4ck^2]\}. \quad \text{(A15)}$$

In fact, the procedure of obtaining the latter equation can be justified only if the dimensionless parameter $LK^2/4k$ is large.

This condition is obviously violated in the high-frequency limit $K/2k \to 0$, hence the approximation (A15) cannot be suitable for the description of directed waves. On the other hand, in the situation we are interested in here, namely, when the radiation wavelength is comparable with the correlation scale of the disorder, the approximation used cannot disturb essentially the accuracy of the final result, since in this case not too much energy of the spectrum $\Phi_\varepsilon(\mathbf{K})$ is concentrated near the origin of the Fourier space. Moreover, as is seen from the latter equation, this does not affect the final result also because the difference of the two terms tends to zero for small arguments.

At the next step, we increase the size of the system by setting formally $L \to \infty$ (this means actually a transfer to a plane wave expansion) while keeping the value of ΩL finite. Mathematically this is possible due to the factor $\cos(\tau \mathbf{K}\cdot\mathbf{k}/k)$ which becomes highly oscillatory for large τ. For directed waves, vector $\mathbf{K}$ is not only small but is always perpendicular to the direction of wave propagation, and transfer to infinite L cannot be validated. For diffuselike waves, however, the fraction of such scattering events is vanishingly small, and, therefore, we can neglect the contributions of the τ/L terms with respect to unity, and extend the upper limit of the integral to infinity. By changing also the integration variable as $\tau = 2kx/K$ we finally obtain Eq. (3.16) of the main text.

APPENDIX B

It is convenient to calculate the two terms constituting the filtering function

$$f(K,\omega,\Omega) = f_1(K,\omega,\Omega) - f_2(K,\omega,\Omega) \tag{B1}$$

separately. The first term, after integrating over azimuthal angle, is of the form

$$f_1(K,\omega,\Omega) = k\frac{2}{\pi}\int_0^\infty dx \cos(xK)\int_0^\pi d\theta \sin\theta \cos(2kx\cos\theta). \tag{B2}$$

The integration over θ leads to a spherical Bessel function $\mathrm{sinc}(2kx)$ and Eq. (B2) is reduced to the step function

$$f_1(K,\omega,\Omega) = \vartheta(2k-K). \tag{B3}$$

The second term reads

$$f_2(K,\omega,\Omega) = k\exp(i\Omega LK^2/8ck^2)\frac{2}{\pi}\int_0^\infty dx\,\mathrm{sinc}(xK) \times \int_0^\pi d\theta \sin\theta\cos(2kx\cos\theta) \times \exp[-i\Omega L(K/4ck)\cos\theta]. \tag{B4}$$

Presenting the cosine as a half-sum of two imaginary exponents and performing the integration over θ leads to

$$f_2(K,\omega,\Omega) = k\exp(i\Omega LK^2/8ck^2)\frac{2}{\pi}\int_0^\infty dx\,\mathrm{sinc}(xK) \times [\mathrm{sinc}(2kx+\Omega LK/4ck) + \mathrm{sinc}(2kx-\Omega LK/4ck)]. \tag{B5}$$

Replacing each of the two sinc functions in the square brackets by an auxiliary integral as

$$\mathrm{sinc}x = \int_0^1 d\xi \cos(x\xi), \tag{B6}$$

we arrive at

$$f_2(K,\omega,\Omega) = (2k/K)\exp(i\Omega LK^2/8ck^2) \times \int_0^1 d\xi \cos(\Omega LK\xi/4ck) \times \frac{2}{\pi}\int_0^\infty dx x^{-1}\sin(xK)\cos(2kx\xi). \tag{B7}$$

Since the internal integral gives the step function $\vartheta(K-2k\xi)$, the remaining integration is trivial and we have

$$f_2(K,\omega,\Omega) = \exp(i\Omega LK^2/8ck^2)\frac{\sin[\Omega L(K/8ck^2)\min(K,2k)]}{\Omega LK^2/8ck^2}. \tag{B8}$$

Finally, combining the two terms of the filtering function we obtain Eq. (3.20) of the main text.

[1] A. Ishimaru, *Wave Propagation and Scattering in Random Media* (Academic, New York, 1978).
[2] M. Fink *et al.*, Rep. Prog. Phys. **63**, 1933 (2000).
[3] M. I. Charnotskii, J. Gozani, V. I. Tatarskii, and V. U. Zavorotny, in *Progress in Optics*, edited by E. Wolf (North-Holland, Amsterdam, 1993), Vol. XXXII, pp. 203–266.
[4] I. Sreenivasiah, A. Ishimaru, and S. T. Hong, Radio Sci. **11**, 775 (1976).
[5] S. Frankenthal, J. Acoust. Soc. Am. **85**, 104 (1989).
[6] A. V. Morozov, J. Opt. Soc. Am. A **19**, 2074 (2002).
[7] G. Samelsohn and V. Freilikher, Phys. Rev. E **65**, 046617 (2002).
[8] *Scattering and Localization of Classical Waves in Random Media*, edited by P. Sheng (World Scientific, Singapore, 1990).
[9] L. A. Apresyan and Yu. A. Kravtsov, *Radiation Transfer: Statistical and Wave Aspects* (Gordon and Breach, Amsterdam, 1996).
[10] Yu. N. Barabanenkov and V. D. Ozrin, Phys. Lett. A **206**, 116 (1995); Yu. N. Barabanenkov, in *Wave Scattering in Complex Media: From Theory to Applications*, edited by B. A. van Tiggelen and S. E. Skipetrov (Kluwer, Dordrecht, 2003).
[11] P. W. Anderson, Phys. Rev. **109**, 1492 (1958).
[12] H. Cao, Y. G. Zhao, S. T. Ho, E. W. Seelig, Q. H. Wang, and R. P. H. Chang, Phys. Rev. Lett. **82**, 2278 (1999).

[13] D. S. Wiersma, M. P. van Albada, B. A. van Tiggelen, and A. Lagendijk, Phys. Rev. Lett. **74**, 4193 (1995).
[14] M. Haney and R. Snieder, Phys. Rev. Lett. **91**, 093902 (2003).
[15] G. Samelsohn and R. Mazar, Phys. Rev. E **54**, 5697 (1996).
[16] G. Samelsohn, S. A. Gredeskul, and R. Mazar, Phys. Rev. E **60**, 6081 (1999).
[17] G. Samelsohn and V. Freilikher, Phys. Rev. E **70**, 046612 (2004).
[18] V. M. Podgaetsky, S. A. Tereshchenko, A. V. Smirnov, and N. S. Vorob'ev, Opt. Commun. **180**, 217 (2000).
[19] L. Wang, P. P. Ho, C. Liu, G. Zhang, and R. R. Alfano, Science **253**, 769 (1991).
[20] D. Huang *et al.*, Science **254**, 1178 (1991).
[21] V. I. Klyatskin, *Stochastic Equations through the Eye of the Physicist* (Elsevier, Amsterdam, 2005).
[22] V. Fock, Phys. Z. Sowjetunion **12**, 404 (1937).
[23] J. M. Cowley, *Diffraction Physics*, 3rd ed. (Elsevier, Amsterdam, 1995).
[24] E. Wolf, in *Trends in Optics*, edited by A. Consortini (Academic, San Diego, 1996).
[25] S. Torquato, Ind. Eng. Chem. Res. **45**, 6923 (2006).
[26] J. C. J. Paasschens, Phys. Rev. E **56**, 1135 (1997).
[27] R. Elaloufi, R. Carminati, and J.-J. Greffet, J. Opt. Soc. Am. A **21**, 1430 (2004).
[28] Z. Q. Zhang, I. P. Jones, H. P. Schriemer, J. H. Page, D. A. Weitz, and P. Sheng, Phys. Rev. E **60**, 4843 (1999).
[29] P. Sebbah, R. Pnini, and A. Z. Genack, Phys. Rev. E **62**, 7348 (2000).
[30] I. M. Vellekoop, P. Lodahl, and A. Lagendijk, Phys. Rev. E **71**, 056604 (2005).
[31] R. Landauer and M. Büttiker, Phys. Rev. B **36**, 6255 (1987).
[32] G. Samelsohn and E. Gruzdev, Phys. Rev. E **78**, 036601 (2008).